sciendo

Quantum-chemical study of the active sites of camptothecin through their Cu(II) coordination ability

Marek Štekláč, Martin Breza

Department of Physical Chemistry, Faculty of Chemical and Food Technology STU, Radlinského 9, 812 37 Bratislava, Slovakia
msteklac@gmail.com

Abstract: The structures of camptothecin (CPT) lactone form and its complexes with Cu(II) were optimized at B3LYP/6-311G* level of theory. Their electronic structures were evaluated via QTAIM topological analysis of electron density and Mulliken population analysis. Stability, electron density distribution and geometrical factors of the optimized systems were compared. Both CPT nitrogen atoms show lower affinity to Cu(II) compared to the oxygen ones. Both the oxygen atom in the CPT lactone ring and the one in the neighbouring carbonyl group show the highest affinity to Cu(II) and the highest stability of Cu-CPT complexes which indicates the most probable CPT reaction sites.

Keywords: B3LYP geometry optimization, camptothecin, population analysis, topological analysis of electron density

Introduction

Camptothecin (CPT), (S)-4-ethyl-4-hydroxy-1H-pyrano [3',4':6,7]-indolizino-[1,2-b]-quinoline-3,14-(4H,12H)-dione, was first discovered in 1966 by M. E. Wall and M. C. Wani while screening naturally occurring products for anticancer effects. It was isolated from the bark and stem of *Campthotheca acuminata*, a tree native to China [Wall at el., 1966; Hsiang and Liu, 1988; Carbonero and Supko, 2002]. Camptothecin inhibits enzyme topoisomerase I, and its derivatives are used in the pharmaceutical industry. It naturally occurs in two forms, which are both stable at different pH ranges. The lactone form (Fig. 1), which is biologically active and thus is the target of our study, is stable at pH < 5.5 and the biologically inactive carboxylic form is stable at pH > 9. The lactone form undergoes hydrolysis under biological conditions, thus transforming into the carboxylic form. Equilibrium of this transformation is achieved after 2 hours and the equilibrium concentration of the lactone form is around 5 % [Kohn and Pommier 2000, Mi and Burke 1994]. The low equilibrium concentration of the lactone form, as well as high affinity of the carboxylic form to human serum albumin, is among the main reasons [Burke and Mi 1994] why camptothecin is not used in the pharmaceutical industry on its own.

Sanna et al. [Sanna et al., 2009] investigated UV–Vis absorption spectrum of ca 5 μM CPT in DMSO-aqueous solutions in a critical 300—400 nm region both experimentally and theoretically. Quantum chemical calculations were performed using B3LYP functional with 6-31G* basis set. Solvent effects were evaluated using Conductor-like Polarizable Continuum Model (CPCM).

Dvoranová et al. [Dvoranová et al., 2013] studied UV–Vis absorption spectrum of 50 μM CPT in various solutions. Geometry optimizations of the CPT lactone monomer and of its head-to-tail π-dimer in six solvents were performed using B97D/cc-pVDZ treatment and solvent effects were approximated within Integral Equation Formalism Polarizable Continuum Model (IEFPCM).

Lesueur-Ginot et al. [Lesuer-Ginot et al., 1999] investigated homocamptothecin (hCPT), a synthetic analogue to CPT with a methylene spacer inserted between an alcohol functional group and a carboxylic group. This E-ring modification (see Fig. 1) leads to lower reactivity and strengthened stability of hCPT. Biological testing revealed that while CPT inhibits topoisomerase I, hCPT enhanced its effect leading to higher levels of DNA cleavage than in the presence of CPT.

This study is aimed to compare the toxicity of possible reaction sites, i.e. the heteroatoms in camptothecin based on their ability to form bonds with copper(II) ion. This method is used to quantify the electron density transfer and spin density transfer from CPT molecule to Cu(II) ion. The authors of this method [Alagona and Ghio, 2009a; Alagona and Ghio, 2009b; Mammino, 2013] have shown that upon coordination the spin density of copper ion decreases while the spin density on the ligand (CPT in our case) approaches 1. In other words, Cu(II) is reduced to Cu(I) while the ligand is oxidized. Consequently, the charge and the spin density of copper can be used to measure affinity of the CPT

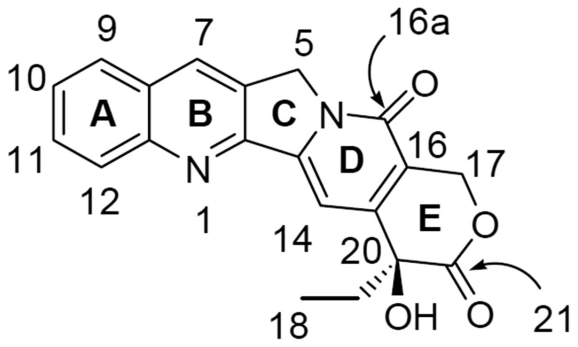

Fig. 1. Atom numbering of camptothecin in a neutral lactone form.

active sites. The extent of electron density transfer between Cu(II) ion and CPT molecule can be evaluated calculating the Laplacian of electron density at Cu—N/Cu—O bond critical points [Puškárová and Breza, 2016; Puškárová and Breza, 2017].

Method

The geometries of the neutral CPT lactone molecule in singlet spin state and its complexes with copper(II) ion in doublet spin state were optimized at B3LYP level of theory [Becke, 1993; Lee et al., 1988]. Standard basis set 6-311G* of Gaussian library [Frisch et al., 2003; Frisch et al., 2009] was used and the stability of optimized geometries were confirmed using vibrational analysis (no imaginary frequencies). The list of optimized systems with their notations used in this paper can be found in Table 1. It should be noted that two initial Cu positions relative to every nitrogen atom in CPT rings (above and perpendicular to their plane) were considered. Interaction energy was calculated as

$$E_{int} = E_{complex} - E_{Cu(II)} - E_{CPT} \quad (1)$$

where $E_{complex}$ is the DFT energy of the $^2[CPT\cdots Cu]^{2+}$ complex, $E_{Cu(II)}$ is the DFT energy of copper(II) ion and E_{CPT} is the DFT energy of the neutral CPT molecule. Charges and spin densities of copper atoms in our systems were evaluated using Mulliken population analysis (MPA) [Mulliken, 1955a; Mulliken, 1955b]. All calculations were done in vacuum, using GAUSSIAN03 [Frisch et al., 2003] and GAUSSIAN09 [Frisch et al., 2016] software packages. Electron transfer between copper ion and initially coordinating heteroatom was evaluated in terms of Quantum Theory of Atoms-in-Molecules (QTAIM) [Bader, 1990] as the Laplacian of the electron density at bond critical points ($\Delta\rho_{BCP}$) and the spin density of copper ion using AIM2000 software [Biegler-König et al., 2001]. MOLDRAW software [Ugliengo, 2006] was used for geometry manipulation and visualisation purposes.

Tab. 1. Notation of the systems under study.

System notation	Initial Cu positions[a)]
A1	$^2[CPT(N_1)\cdots Cu]^{2+}$ [b)]
A2	$^2[CPT\ (N_1)\cdots Cu]^{2+}$ [c)]
A3	$^2[CPT(N_4)\cdots Cu]^{2+}$ [b)]
A4	$^2[CPT(N_4)\cdots Cu]^{2+}$ [c)]
B1	$^2[CPT(O_{16a})\cdots Cu]^{2+}$
B2	$^2[CPT(O_{lactone})\cdots Cu]^{2+}$
B3	$^2[CPT(O_{20})\cdots Cu]^{2+}$
B4	$^2[CPT(O_{21})\cdots Cu]^{2+}$

Remarks:

[a)]coordinating heteroatoms in parentheses (see Fig. 1 for atoms notation)

[b)]above the CPT rings plane

[c)]perpendicular to the CPT rings plane

Results and discussion

Geometry optimizations of eight starting $^2[CPT\cdots Cu]^{2+}$ complexes resulted into six stable structures (for their molecular graphs see Figs. 2—7).

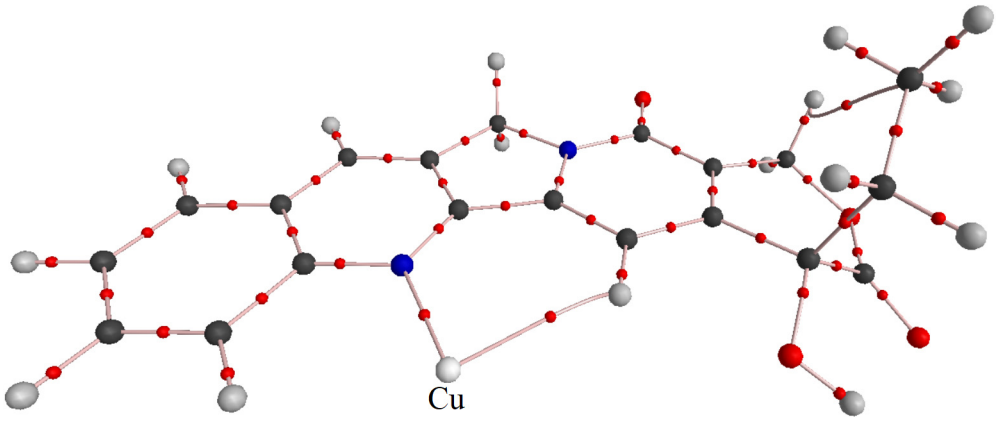

Fig. 2. Molecular graph of the optimized geometry of systems A1 and A2 (black — carbon, white — hydrogen, blue — nitrogen, red — oxygen, small red — bond critical point).

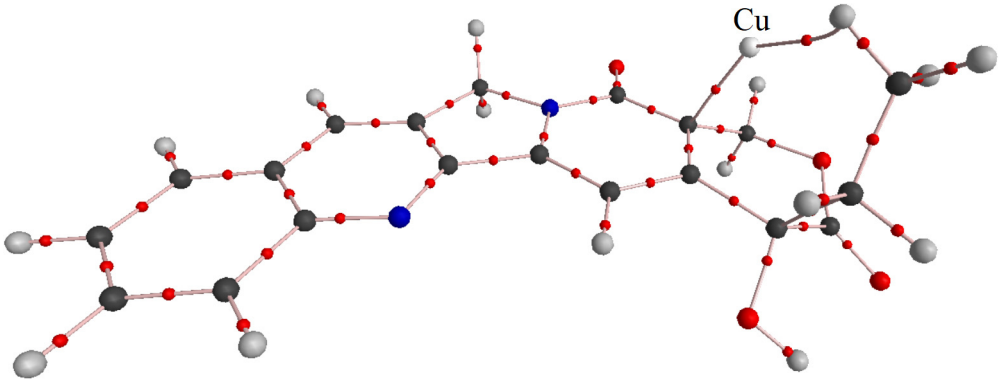

Fig. 3. Molecular graph of the optimized geometry of system A3 (black — carbon, white — hydrogen, blue — nitrogen, red — oxygen, small red — bond critical point).

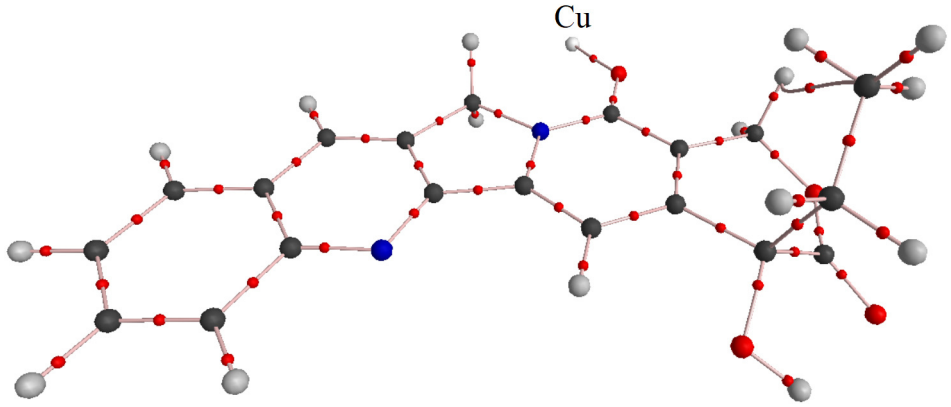

Fig. 4. Molecular graph of the optimized geometry of system A4 (black — carbon, white — hydrogen, blue — nitrogen, red — oxygen, small red — bond critical point).

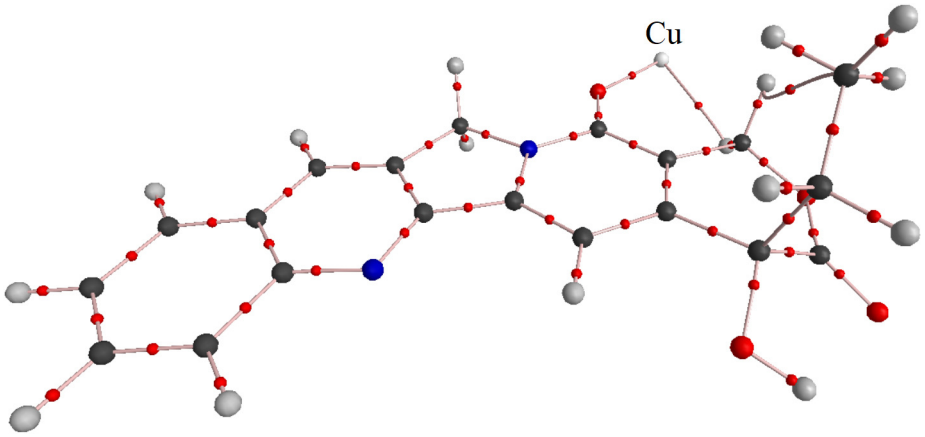

Fig. 5. Molecular graph of the optimized geometry of system B1 (black — carbon, white — hydrogen, blue — nitrogen, red — oxygen, small red — bond critical point).

Our results (see Table 2) indicate that the most stable complexes (i.e. with the lowest interaction energy) were formed when copper was coordinated either by oxygen in the lactone ring or by oxygen on carbon C_{21} (systems B4 and B2). It should be noted that after geometry optimization both these initial geometries resulted into the same structure, in which copper was coordinated by oxygen on carbon C_{21} (system B2 transformed into B4, see Fig. 6). The same was observed for systems A1 and A2 where copper ion was coordinated by N_1 (see Fig. 2). The least stable complexes were formed with N_4 in both initial configurations (systems A3 and A4, see Fig. 3 and Fig. 4). This fact can be explained by steric effects of nearby atoms/functional groups. This conclusion is further illustrated by the distance of

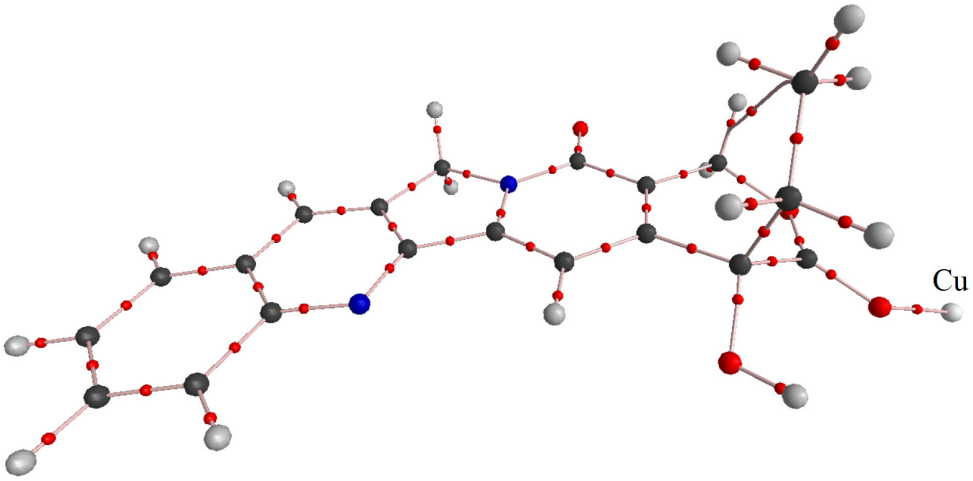

Fig. 6. Molecular graph of the optimized geometry of systems B2 and B4 (black — carbon, white — hydrogen, blue — nitrogen, red — oxygen, small red — bond critical point).

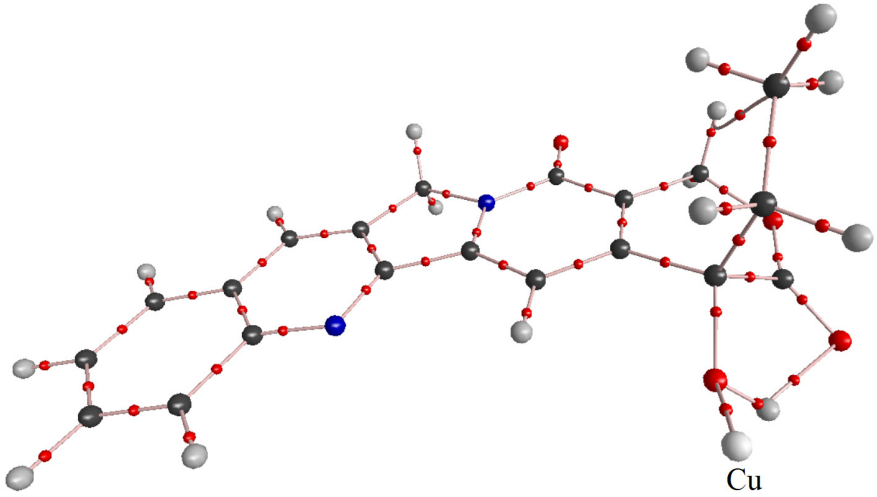

Fig. 7. Molecular graph of the optimized geometry of system B3 (black — carbon, white — hydrogen, blue — nitrogen, red — oxygen, small red — bond critical point).

Tab. 2. Calculated Cu-heteroatom distances (d), interaction energies (E_{int}), MPA Cu charges and spin densities, QTAIM Cu charges, spin densities and Laplacians of the electron density at bond critical points of Cu···X bonds ($\Delta\rho_{BCP}$) of the systems under study.

System	A1[a)]	A2[a)]	A3	A4	B1	B2[b)]	B3	B4[b)]
Heteroatom (X)	N_1	N_1	N_4	N_4	O_{16a}	$O_{lactone}$	O_{20}	O_{21}
d(Cu···X) [Å]	1.888	1.888	3.562	3.442	1.858	3.008	1.907	1.872
E_{int} [kJ mol^{-1}]	–1158.45	–1158.45	–1112.53	–1120.41	–1135.74	–1193.08	–1132.01	–1193.08
MPA characteristics								
Cu charge	0.907	0.907	0.953	0.904	0.917	0.857	0.909	0.857
Cu spin	0.001	0.001	0.043	0.014	0.013	0.000	0.000	0.000
QTAIM characteristics								
Cu charge [e]	0.821	0.821	0.753	0.919	0.911	0.914	0.892	0.914
Cu spin density [e Bohr^{-3}]	0.003	0.003	–0.190	0.015	0.032	0.003	0.000	0.003
$\Delta\rho_{BCP}$ [e Bohr^{-5}]	0.507	0.507	–[c)]	–[c)]	0.646	–[c)]	0.567	0.628

Remarks:

[a)]systems A1 and A2 lead to the same optimized geometry

[b)]systems B1 and B4 lead to the same optimized geometry

[c)]bond critical point between copper ion and the initial heteroatom was not found

copper atom from the initial heteroatom in the optimized geometries (Table 2). The highest electron transfer corresponding to the highest Laplacians of the electron density at bond critical point between copper ion and the coordinating heteroatom was observed in systems with copper ion coordinated by oxygen on carbon $C_{16\text{-}a}$ (system B1, see Fig. 5) and in the previously mentioned system B4 (see Fig. 6). On the contrary to MPA data, QTAIM analysis indicates the lowest spin density and the lowest charge of copper ion in systems with copper coordinated by oxygen on carbon C_{20} (system B3) and in the previously mentioned system B4.

Conclusion

The aim of this study was to quantify and subsequently compare the toxicity of active sites in the camptothecin lactone form through the method of copper(II) ion probe [Alagona and Ghio, 2009a; Alagona and Ghio, 2009b; Mammino, 2013; Puškárová and Breza, 2016; Puškárová and Breza, 2017]. We have shown that both nitrogen atoms in the CPT structure are inactive and we have concluded that the heteroatom with the highest affinity to Cu(II) (as the model of radicals) in camptothecin is oxygen on carbon C_{21}. Furthermore, we have demonstrated that substitutions on oxygen in the lactone ring lead to geometry identical to the substitution on the aforementioned oxygen. This result, combined with the biological activity of the lactone form of CPT presents the basic ideas about the mechanism of its reaction with topoisomerase I. The QTAIM results are in an excellent agreement with the concept that CPT binds to topoisomerase I with three hydrogen bonds formed by oxygen atom in the lactone ring, oxygen on carbon C_{21} and by alcohol moiety on carbon C_{20} [Redinbo et al., 1998].

Obtained results can be further used to shed more light on the reactions of camptothecin and its derivatives in human body. Our results can be used in the target synthesis of new CPT derivatives and as part of a more complex study of camptothecin in its various forms.

Acknowledgments

This work was supported by the Slovak Grant Agency VEGA (contract no. 1/0598/16) and by the Slovak Science and Technology Assistance Agency (contract no. APVV-15-0079).

References

Alagona G, Ghio C (2009) J. Phys. Chem. A 113: 15206–15216.

Alagona G, Ghio C (2009) Phys. Chem. Chem. Phys. 11: 776–790.

Bader RFW (1990) Atoms in Molecules: A Quantum Theory, Claredon Press, Oxford.

Becke AD (1993) J. Chem. Phys. 98: 5648–5652.

Biegler-König F, Schönbohm J, Bayles D (2001) J. Comput. Chem. 22: 545–549. Available from: http://www.aim2000.de.

Burke TG, Mi Z (1994) J. Med. Chem. 37: 40–46.

Carbonero RG, Supko JG (2002) Clin. Cancer Res. 8: 641.

Dvoranova D, Bobeničová M, Šoralová S, Breza M (2013) Chem. Phys. Lett. 580: 141–144.

Frisch MJ, Trucks GW, Schlegel HB, Scuseria GE, Robb MA, Cheeseman JR et al. (2003) Gaussian 03, Revision. C1, Gaussian, Inc., Pittsburgh PA.

Frisch MJ, Trucks GW, Schlegel HB, Scuseria GE, Robb MA, Cheeseman JR et al. (2016) Gaussian 09, Revision A.02, Gaussian, Inc., Wallingford CT.

Hsiang YH, Liu LF (1988) Cancer Res. 48: 1722–1726.

Kohn KW, Pommier Y (2000) Ann. N. Y. Acad. Sci. 922: 11–26.

Lee Ch, Yang W, Parr RG (1988) Phys. Rev. B 37(2): 785–789.

Lesueur-Ginot L, Demarquay D, Kiss R, Kasprzyk PG, Dassonneville L, Bailly C, Camara J, Lavergne O, Bigg DC (1999) Cancer Res. 59(12): 2939–2943.

Mammino L (2013) J. Mol. Model. 19: 2127–2142.

Mi Z, Burke TG (1994) Biochemistry 33: 10325–10336.

Mulliken RS (1955) J. Phys. Chem. 23: 1833–1840.

Mulliken RS (1955) J. Phys. Chem. 23: 1841–1846.

Puškárová I, Breza M (2016) Polym. Degrad. Stab. 128: 15–21.

Puškárová I, Breza M (2017) Chem. Phys. Let. 680: 78–82.

Redinbo MR, Stewart L, Kuhn P, Champoux JJ, Hol WGJ (1998) Science 279(5356): 1504–1513.

Sanna N, Chillemi G, Gontrani L, Grandi A, Mancini G, Castelli S, Zagotto G, Zazza C, Barone V, Desideri A (2009) J. Phys. Chem. 113(16): 5369–5375.

Ugliengo P (2006) MOLDRAW: a Program to Display and Manipulate Molecular and Crystal Structures, Torino. Available from: http://www.moldraw.unito.it.

Wall ME, Wani MC, Cook CE, Palmer KH, McPhail HT, Sim GA (1966) J. Am. Chem. Soc. 88: 3888–3890.